Predominant-period Site Classification for Response Spectra Prediction Equations in Italy

by Carola Di Alessandro, Luis Fabian Bonilla, David M. Boore, Antonio Rovelli, and Oona Scotti

Abstract

We propose a site classification scheme based on the predominant period of the site, as determined from the average horizontal-to-vertical (H/V) spectral ratios of ground motion. Our scheme extends Zhao et al. (2006) classifications by adding two classes, the most important of which is defined by flat H/V ratios with amplitudes less than 2. The proposed classification is investigated by using 5%-damped response spectra from Italian earthquake records. We select a dataset of 602 three-component analog and digital recordings from 120 earthquakes recorded at 214 seismic stations within an hypocentral distance of 200 km. Selected events are in the moment-magnitude range $4.0 \leq Mw \leq 6.8$ and focal depths from a few kilometers to 46 km. We computed H/V ratios for these data and used these to classify each site into one of six classes. We then investigate the impact of this classification scheme on empirical ground-motion prediction equations by comparing its performance with that of the conventional rock/soil classification. Although the adopted approach results in a only a small reduction of overall standard deviation, the use of H/V spectral ratios in site classification does capture the signature of sites with flat frequency-response, well as deep and shallow soil profiles, characterized by long- and short-period resonance, respectively; in addition, the classification scheme is relatively quick and inexpensive, which is an advantage over schemes based on measurements of shear-wave velocity.

Introduction

Ground-motion prediction equations (GMPEs) are a fundamental tool in seismic hazard assessment. For the same magnitude and distance, however, variations due to site conditions can be very large and must be properly taken into account in deriving coefficients of the GMPEs. Many recent GMPEs use the value of shear wave velocity in the uppermost 30 m (V_{S30}) to assign sites to a few classes. Table 1 gives the definitions of two commonly used sets of classes: the American (NEHRP, 2000) and European (CEN, 2004) classes. These velocity-based classifications do have some problems, not least of which is the limited availability of near-surface shear-wave models at strong-motion sites in many countries. In addition, the cost of obtaining the information can be quite high, especially if based on borehole measurements. A more affordable alternative are velocity profiles inferred from dispersion curves, but they are strictly applicable to 1D situations (see Xia *et al*., 2002; Di Giulio *et al*., 2006; Boore and Asten, 2008). Even if V_{S30} values are available, however, the site classes based on these values do not capture the role of the thickness of soft sediments (Steidl, 2000), nor do they capture site resonances in narrow period bands. The limitation of V_{S30} classes is particularly relevant in deep basins where predictions based on V_{S30} may overestimate amplitudes at short periods and underestimate long periods (Park and Hashash, 2004). Including the depth of the uppermost resonant layer in site classification has been recently proposed by Rodriguez-Marek *et al*. (2001) and Pitilakis et al. (2006). Cadet *et al*. (2010) investigate whether combining V_{S30} and the fundamental resonance frequency (f_0) is a better way of characterizing sites than using V_{S30} alone. The fundamental frequency of the resonant layer has been used as well by Luzi *et al*. (2011) to propose a site classification for Italian stations.

An alternative to V_{S30}-based classes was proposed by Zhao *et al*. (2006), based only on the site predominant period inferred from H/V spectral ratios. This criterion is used in Japan for the seismic design of highway bridges (Japan Road Association, 1980 and its 1990 revision).

Fukushima *et al*. (2007) applied Zhao's classification scheme to a database composed primarily of European earthquakes with a partial contribution of near-source Californian and Japanese earthquakes; the stations that provided the data had originally been classified as rock or soil. While Fukushima *et al*. (2007) were able to unambiguously classify 64 % of the total stations, they expressed some concerns on whether there were enough stations that represented the classes that amplify intermediate periods. More recently, a study performed by Ghasemi *et al*. (2009) tested the feasibility of Zhao's classification scheme on Iranian strong-motion stations, attempting three different automatic classification methods but maintaining the same period-range subdivision among the various site classes.

In this paper, we adopt the site-classification method used by Zhao *et al*. (2006) and Fukushima *et al*. (2007), with a few changes. The main difference is the introduction of a new class characterized by flat H/V spectral ratios with amplitudes less than 2. This new class helps in the recognition of reference rock sites. We apply our site classification to the strong-motion stations of the Italian Accelerometric network (RAN), managed by the Italian Department of Civil Protection (DPC). In addition to assigning a predominant period class to each recording site, we also classify each site as rock or soil, based on available geotechnical and geological information. The available information for the station characterization presents different refinements levels: it varies from measurements of Vs at 102 sites (45 using cross-hole or down-hole invasive measurements, and 57 using non-invasive methods) in the best cases (Di Capua *et al*., 2011), to subjective characterization based on geological considerations in the worst cases. Our study is part of a research project, sponsored by the Department of Civil Protection of Italy (S4 Project, http://esse4.mi.ingv.it), to investigate alternatives to the conventional V_{S30} criteria, with the goal of providing a more homogeneous description of geotechnical and

geophysical features at each station to be included as metadata in the strong-motion database (ITACA, Italian Accelerometric Archive, http://itaca.mi.ingv.it).

In this paper we first present the proposed site classification scheme and use the scheme to classify many sites in Italy that recorded earthquake motions. We then evaluate the new model by applying regression analysis in order to derive GMPEs and to study the related errors. Comparison with predicted spectra based both on predominant-period and conventional classification criteria are also shown. Finally, we discuss to what extent recorded data from the April 6, 2009, L'Aquila earthquake are matched by our proposed GMPEs (our GMPEs were derived using earlier data); we find that the site class variations for the L'Aquila earthquake are consistent with those predicted from our GMPEs. This suggests that the site classification scheme is stable and useful.

Proposed Site Classification

Zhao *et al*. (2006) and Fukushima *et al*. (2007) proposed a classification criterion based on the predominant period of each station identified through the average H/V spectral ratio of the 5%-damped response spectra. In this paper, we apply a similar classification criterion to the Italian dataset.

Our predominant period classification scheme consists of seven classes. The first four classes (CL-I to CL-IV) are the same as those defined by Zhao *et al*. (2006) (Table 2). We further introduce three classes to take into account stations that could not be classified as a function of a unique peak in H/V. Independently of the originally available site-category description in terms of geological setting and/or geophysical parameters, we classify a station as generic rock (CL-V) if it displays an almost flat average H/V response spectral ratio with no clear peak and a small overall H/V ratio (< 2), whereas we classify it as generic soft soil (CL-VI) if there is a broad amplification at periods longer that 0.2 s or if there is more than one peak and all peaks occur at periods longer than 0.2 s. If multiple peaks are present both before and after the 0.2 s period threshold, the station cannot be unambiguously classified and therefore it is referred to as "unclassifiable" (CL-

VII). Figure 1 shows examples of stations that were classified according to our proposed classification scheme.

In addition to the classifications based on the predominant-period, we also used the geologic information to place each site into one of two classes based on the European (CEN, 2004) classification (where we have lumped A and B and C and D classes together): AB and CD ($V_{S30} \geq 360$ m/s and $V_{S30} < 360$ m/s, respectively; see Table 3). The few sites of class E, as defined in CEN (2004), were included in the AB category. In this way, each site has been classified on the basis of its predominant period and of its resemblance to rock (AB) or soil (CD).

Data Used

We study the proposed site classes by using the available digital and digitized analog accelerograms of Italian earthquakes from 1972 to 2004 collected in ITACA strong-motion database (Luzi et al., 2008; Pacor et al., 2011). Additional accelerometric signals for selected recent (2005-2008) events with Mw > 4.0 were also included. We supplemented the accelerograms with a small percentage (4%) of broad-band velocity-sensor seismograms (converted to acceleration time series via differentiation for the computation of response spectra). The addition of ground motions derived from broad-band seismograms helps to better constrain ground motions at distances larger than 100 km, where some GMPEs (e.g. Sabetta and Pugliese, 1996; Bindi *et al*., 2010) in use for the Italian territory are not applicable, because of the small number of accelerograms available at those distances before the April 2009, L'Aquila earthquake.

After the removal of some stations that were suspected of having soil-structure interaction (see Deliverable D8 of the aforementioned Project S4, available at http://esse4.mi.ingv.it/), the time series and Fourier spectra were carefully inspected to make sure that the strongest part of the motions was well recorded and that the signal/noise ratio was acceptable in the frequency range 0.5 to 20 Hz. The final dataset consists of 602 three-component digital and analog recordings from 120 earthquakes

recorded at 214 seismic stations within hypocentral distances of 200 km. The moment-magnitudes (Mw) range from 4.0 to 6.8. The largest events have focal depths in the range 5 to 32 km; only one earthquake was deeper (46 km), and it was included in the analysis because its spectral ordinates were consistent in shape and amplitude with those from the shallower earthquakes. Some of the smaller events were at depths less than a few kilometers. The distribution of the records versus magnitude and hypocentral distance is shown in Figure 2.

About 50% of the dataset are from the Friuli, Irpinia, Umbria-Marche, and Molise earthquakes, whose mainshocks had Mw magnitudes of 6.4 (Pondrelli *et al*. 2001), 6.8 (Cocco and Rovelli, 1989), 6.0 (Ekström *et al*., 1998), and 5.7 (Chiarabba *et al*., 2005), respectively.

All signals were pre-processed to remove the pre-event mean from the whole record (the zeroth-order correction as defined in Boore *et al*., 2002; the whole-record mean was used if no pre-event portion was available). A Butterworth fourth-order acausal high-pass filter was then applied to signals after cosine tapering and zero-padding both at the beginning and the end (Boore, 2005, and Boore and Bommer, 2005). The length of the zero-padding depends on the order of the filter and on the cut-off frequency according to Converse and Brady (1992). In order to maintain a consistent filtered dataset and to reduce the influence of the filter cut-off on the usable frequency range, we chose to use response spectra for periods less than 2 s; this period is 70% of the minimum cut-off period used in the filters (Abrahamson and Silva, 1997, and Spudich *et al*., 1999). Although Paolucci *et al*. (2008) demonstrated that digital accelerograms provide reliable response spectra up to longer periods, the choice of a 2 s upper limit is conservative and conditioned by the use of many analog records (including analog records is necessary if the largest magnitude events in Italy are included in our dataset, as these events were only recorded on analog instruments).

Results of Classifying Italian Strong-Motion Stations

We assigned a classification based on predominant period for all 214 selected stations. We used the complete dataset for the regression computation, but we considered a subset of 111 stations that recorded more than one event for statistical purposes (see Tables 4 and 5, and Figures 3a and 3b). The determination of the predominant period of each station was made after computing the average H/V spectral ratio over the events recorded at the station (or over the two horizontal components treated as independent in the case of stations that only recorded a single event). We used ratios of response spectra rather than Fourier spectra (as in Yamazaki and Ansary, 1997) because they do not need subjectively chosen smoothing. The dominant period was determined using the identification procedure proposed by Zhao *et al*. (2004), based on a quadratic function fit to the H/V spectral ratios at three samples around the peak. At the end of this process, we visually inspected the results, and we manually classified some stations for which Zhao's identification procedure gave ambiguous results.

The statistics of the classifications are summarized in Tables 4 and 5, which show cross-tabulation of the stations into the two sets of site classes. Most "rock-like" AB sites correspond to the new categories CL-I and CL-II, although some are in the more "soil-like" classes CL-IV and CL-VI. Similarly, "soil-like" CD sites fall into all but the CL-V classes, with the CL-IV class being the most common. Note that we were able to classify 79 sites out of 91 AB sites and 18 sites out of 20 CD sites using the predominant period criterion (87% in total, Table 4). The percentage of successful classifications in terms of numbers of records is similar (89%, Table 5).

We computed the geometric mean H/V response spectral ratio and its standard deviation for each site class (Figure 3a and 3b). The shape of the mean H/V response spectral ratios are comparable to the results obtained by Zhao *et al*. (2006) for data from Japanese stations (see their Figure 3a and 3b), at least for the common classes: the periods of the peaks in the mean spectral ratios are consistent with what they found, that is around 0.15 sec, 0.25 sec, 0.4 sec, and 0.8 sec for CL-I, CL-II, CL-III, and CL-IV sites, respectively (of course, given that entries in each class are based on the predominant

period, it is no surprise that the peaks of the mean ratios are consistent with the site class definitions). As expected on the basis of the class definitions, class CL-V exhibits an almost flat mean H/V response spectral ratio, as we expect for generic rock sites, while class CL-VI displays a broader mean H/V response spectral ratio shape without predominant peaks. The standard deviations have reasonably small values, ranging from 0.2 in natural logarithm scale for class CL-V up to about 0.4 for all the other classes but CL-IV (Figure 3b). The standard deviation for the latter class is about 0.7 at 0.9-sec period. The analysis of the skewness reveals that this high standard deviation value is due to few sites characterized by very high H/V spectral ratios, up to 16, for stations located in basins like the Aterno Valley and the Po and Garigliano Plains, both characterized by hundreds of meters of alluvial sediments (see De Luca *et al*., 2005, and Malagnini *et al*., 1993, respectively). Apart from class CL-IV, in the remaining classes there is a substantial reduction of our standard deviations (20 - 40 %) compared to the results by Zhao *et al*. (2006) and Fukushima *et al*. (2007), both of whom used a larger dataset. For the sake of example, in the class that amplifies at short period, our study finds standard deviation below 0.4 in natural logarithm scale, whereas both Zhao et al., 2006, and Fukushima et al., 2007, find peak values around 0.5. A similar behavior is noted for the class that amplifies at intermediate period, where our study finds values below 0.35 whereas both Zhao and Fukushima finds values on the order of 0.5 – 0.6.

In order to evaluate whether magnitude and hypocentral distance could cause any bias to the classes assigned to the dataset, we study the variations of the H/V spectral ratios for different magnitude and distance ranges. Table 6 and 7 shows the number of records in each site class for the different groups. The variations of the H/V spectral ratios between different magnitude and distance ranges are in general not significant. Class CL-IV exhibits moderately larger peak ratios for records with Mw between 5.0 and 5.4, in comparison to those of other magnitude ranges, probably because of the particular combination of events and soft-soil stations that recorded these events. However, the shapes of the average H/V spectral ratios in each class are remarkably stable and are the period of the predominant peak does not shift with magnitude, thus implying that nonlinearity does not seem to play an important role in this study. Since variations in amplitude, if any, are not relevant to the purpose of site classification, we can conclude

that there is no magnitude or hypocentral distance dependence for the site classes. (More results are given in Figures E1 and E2 of the electronic supplement).

Application of the Proposed Site Classifications

Our evaluation of the proposed site classifications is based on ground-motion prediction equations fit to the data, both with the new site classes and with the simplified rock/soil classification. The distribution of data from different predominant period classes with respect to moment magnitude and hypocentral distance (Fig. 2) shows that there is no significant bias in the dataset; therefore, we felt confident in performing the regression computation. We adopted the functional form proposed by Fukushima *et al*. (2003), that is

$$\log_{10} Sa(T) = a(T) + b(T)M + c(T)M^2 + d(T)R - \log_{10}\left(R + e(T)^{10 f(T) M}\right) + S_j(T)\delta_j \qquad (1)$$

where $Sa(T)$ is the elastic absolute response spectral acceleration for 5% damping. The functional form (1) includes magnitude saturation at close distances and a quadratic magnitude dependence of the motions at a fixed distance. $Sa(T)$ was computed from the 602 selected records as the geometric mean of the two horizontal components. In equation (1), a, b, c, d, e and S_j are period-dependent regression coefficients, and M and R are moment magnitude and hypocentral distance (in km), respectively. The suffix j corresponds either to the AB and CD classes or to the seven site classes proposed in this study based on the predominant period. A summation of all site classes (except for AB or CL-I classes, which are taken to be the reference conditions for the site response terms $S_j(T)$) is assumed in the term $S_j(T)\delta_j$, and δ_j is a dummy variable, which is equal to 1 if data are observed at j-th site category and 0 otherwise.

Fukushima *et al*. (2003) used a winnowing procedure in their dataset in order to exclude small magnitude events at larger distances. We checked this effect in our dataset and realized that such winnowing does not make a strong difference in terms of overall results and standard deviation. Therefore, in order to keep as much as possible data, we decided to not apply any winnowing as a function of distance and magnitude.

Details of the coefficient computation and comparison with other existing predictive equations at regional and global scale using different site classification criteria are discussed in the Appendix. In that Appendix we find a satisfactory agreement with predictions of other regressions that used much larger data sets; we want to stress, however, that the main goal of this study is not the publication of a new GMPE with a limited regional applicability but a check of our new classification scheme comparing its prediction performance with a conventional classification when the same data and same statistics are used.

Relative amplifications were computed for our classes with respect to a reference class, which was assumed to be the CL-V site class or the AB site class; these amplifications are shown in Figure 4a (although CL-I was chosen as the reference condition in doing the regression, the amplifications can be presented relative to any class; in Figure 4a we have chosen to use CL-V as the reference condition). As shown in that figure, classes CL-I, CL-III, and CL-IV show a comparable amplification factor with respect to CL-V of about 2.5 around 0.13s, 0.35s and above 1s, respectively, whereas CL-II class shows a lower amplification (1.8 at 0.25s). This amplification level is similar to the one attained by CL-VI class, even though the latter maintains a broad amplification up to longer periods. Figure 4a also shows interesting high-frequency amplification for CL-I class. This amplification was also found by Fukushima *et al*. (2007); given that their data were mostly from the western Eurasia area, whereas ours are from Italy, the similarity in the results suggests that the high-frequency CL-I amplification could be a global feature. Figure 4a also shows that the relative amplification of CD class with respect to AB resembles closely the one for CL-IV with respect to CL-V, both in terms of spectral shape and amplitude.

Figure 4b shows relative amplifications between the two types of classes. To compute the predicted relative amplifications for simplified site classes AB and CD with respect to CL-V, we needed to take into account the different magnitude and distance dependencies in the GMPEs for the two ways of classifying sites; therefore, we created a matrix of magnitude-distance couples compatible with our dataset, computed the motions for AB, CD, and CL-V sites, formed the ratios of motions for each magnitude and distance pair, and averaged the ratios over all pairs of magnitude and distance. Figure 4b shows the average ± 1 standard deviation for the predicted relative amplification between AB and CD site classes when CL-V is used as a reference class. Since the AB class includes hard/stiff and shallow soft sites mixed together, Figure 4b shows that, when CL-V is used as the reference, the AB class is amplified up to a factor of 1.5 with a broad shape, and this indicates that the rock class CL-V better captures the main feature of a rock/stiff behavior. Furthermore, relative amplification of the CD class with respect to CL-V has a comparable shape to the one for CD with respect to AB (repeated from Figure 4a to better allow comparison) but displays higher amplitudes.

Figure 5 shows the effect of our proposed predominant period classification on corresponding predicted response spectra, compared to the trend shown by our regression using the simplified AB and CD classification and by the GMPEs of Zhao *et al*. (2006) and Fukushima *et al*. (2007) (these were used because they employ a similar site classification criterion, based on predominant period). For the sake of example we plot spectral ordinates for moment magnitudes Mw 4.5 and 6.0 (panels from the bottom to the top) at a hypocentral distance of 50 km. For each magnitude, response spectra for each site class are grouped in terms of the predominant period used to define the site class (amplification at short-, intermediate- and long periods, for the left, middle, and right columns of graphs, respectively). Considering only our GMPEs, with respect to the original AB site class the predicted response spectrum for CL-V class shows lower values, especially at short periods (up to 1 second). Conversely, the predicted response spectrum for CL-I class displays higher values. It is worth noticing that the predicted response spectrum for CL-I class has the highest peak value. This effect can be due to weathering of rock or the presence of thin soft layers with strong impedance contrast (usually referred to class E in CEN, 2004). With respect to the original CD site class, the

predicted response spectrum for CL-IV class is smaller but maintains a very similar shape. It is typically bimodal, with the longer period lobe that increases in importance as magnitude increases.

In terms of comparisons between GMPEs, Figure 5 indicates that there is satisfactory agreement in the spectral shape of all the GMPEs based on predominant period in H/V spectral ratios, although there are some differences in amplitudes. . The comparison with the Zhao *et al*. (2006) and the Fukushima *et al*. (2007) GMPEs shows fairly good agreement at Mw 6.0, whereas our predicted spectral amplitudes tend to be somewhat lower at Mw 4.5. However, all these variations are less than a factor of 2 and do not exceed the usual uncertainty of 0.3 (log base 10). This is an interesting result if we consider the smaller numbers in the Italian dataset, of the order of hundred records against thousands of Zhao *et al*. (2006). The most noticeable amplitude differences are confined within the classes that amplify at short period. For instance, at Mw 6.0, the amplitudes of SA for our class CL-I are comparable to those for Fukushima *et al*.'s CL-1 but are larger than Zhao *et al*.'s SA for SC-I; in contrast, the latter is in better agreement with our curves for CL-V class at the same Mw 6.0. The peculiar high amplitude at short periods for class CL-I is also evident when comparing predicted spectra with other non-predominant-period based GMPEs (these results are shown in the Appendix Fig. A5).

In order to help judge the impact of the new site classification on predicted response spectra, we evaluated whether and to what extent we can achieve a reduction of uncertainty in ground motion prediction. Overall standard deviation obtained using predominant period classification and original AB-CD site classes in $\log_{10}$ logarithms are compared in Figure 6a. Figure 6a also shows the inter- and intra-event terms deviation as derived from the regression analysis. Although there is a reduction at short periods when using the period-based site classes, it is small (but comparable to that found by Fukushima *et al*. (2007), as shown in Figure 6b). Achieving only a small reduction in the variance with the use of more complex site classes is not unexpected and is not a definitive test of the efficacy of a site classification scheme. In studying a relative small number of motions, Boore (2004) found that the overall variance of individual observations about predicted values decreased only slightly in going from no

classifications to classification based on continuous V_{S30}, with the largest reduction coming from a rock/soil classification to a NEHRP class classification. The more complex schemes, however, did remove systematic trends in the residuals.

In addition, we notice in Figure 6 that the aleatory variation tends to decrease at longer period, opposite to what Fukushima *et al* (2007) found with their regression. With either site classification scheme, our standard deviations are higher than those found in number of other studies. Others have observed this feature of Italian strong-motion data (e.g. Bindi *et al*., 2010; Scasserra *et al*., 2009). Cauzzi and Faccioli (2008) have suggested that the relatively high values of standard deviation at shorter periods could possibly be related to the scatter introduced by site-related amplification effects.

Relative differences in amplifications from the GMPEs and from recordings of the L'Aquila earthquake

We completed the computation of the coefficients in equation (1) before the occurrence of the April 6, 2009, Mw 6.3 L'Aquila earthquake in central Italy (Chiarabba *et al*., 2009, Çelebi *et al*., 2010). It was a normal faulting earthquake that ruptured a 10x25 km^2 fault oriented along the Apennine trend beneath the town of L'Aquila (Cirella *et al*., 2009, Anzidei *et al*., 2009, Atzori *et al*., 2009). Fifty four accelerometers were triggered, with hypocentral distances from 11 to 277 km. These records gave us the opportunity of investigating how the new recorded ground motions compare to the predicted values using the predominant period site classification, including a test on the performance of the site correction terms. Eighteen of the stations that recorded the L'Aquila earthquake had been previously classified in our study; we used the L'Aquila recordings to assign site classes at 36 other stations.

Figure 7 shows the residuals from L'Aquila earthquake for the different site classes. We grouped the residuals according to their hypocentral distance (within or beyond 100 km, respectively) and we show results in terms of PGA and spectral ordinates at two selected periods (0.2 and 1.0 sec). In Figure 7 cross and open circle symbols are used to

distinguish stations whose source-to-station azimuth measured clockwise from north is in the range 57° – 187° and 200° – 330°, respectively. We borrow these ranges from Ameri et al. (2009), who, in common with other studies (Pino and Di Luccio, 2009; Chioccarelli and Iervolino, 2010, Bindi *et al*., 2009a), found increasing ground motion southeast of the epicenter and decreasing motion for stations in the opposite direction (this pattern might be due to directivity associated with the propagation of the mainshock rupture). For the purpose of our study, the most important findings from Figure 7 are the similarities in the mean residuals for each class, thus suggesting that the site effect corrections are proper, as they are not producing class-to-class differences in the residuals. The overall negative residuals for this peculiar earthquake are not of concern, and they have been already reported in other papers that studied the event (e.g., Ameri *et al*., 2009, Akinci *et al*., 2010 and Çelebi *et al*., 2010).

Finally, the average residuals computed for L'Aquila earthquake are similar to the inter-event residuals at Mw 6.3 from our GMPE regression analysis (see Figure A1), so we can argue that adding the April 6, 2009, L'Aquila earthquake to the dataset used to compute the regression coefficients would have had little effect on the regression results.

Conclusions and Discussion

In this paper we present a new site classification scheme for Italian stations, based on the predominant period of the site, as derived from the average horizontal-to-vertical (H/V) spectral ratios of ground motion. This classification scheme is the same as proposed by Zhao *et al*. (2006), with the addition of two classes that account for cases not included in Zhao *et al*. classes. One (which we call CL-V) is defined as a site for which H/V does not exhibit any predominant peaks, with an overall H/V ratio less than 2; the other (CL-VI) also has broad amplifications or multiple peaks in the average H/V ratio at period larger than 0.2 seconds. In addition, we include another class (CL-VII) not included in Zhao *et al*. (2006): a catchall class for any site which cannot be placed in the other sites. We then use the new scheme to classify stations in Italy that recorded strong

motions, and we then derived ground-motion prediction equations (GMPEs) for these motions (GMPEs were also derived using a simple rock/soil classification scheme).

Despite the relatively small reduction of standard deviation at shorter periods when we use the predominant-period classification, our scheme has the advantage of recognizing well distinguished behavior of the proposed classes, both in terms of relative amplification with respect to rock site (i.e. AB or CL-V sites) and of predicted spectral shape.

The new CL-V site is useful to classify rock stations to be used as reference sites in site response studies and in the development of GMPEs. Neither Zhao *et al*. (2006) nor Fukushima *et al*. (2007) included a comparable classification. As a matter of fact, when they were unable to identify a predominant period they used the available geological information to distinguish generic rock or generic soil classes. Fig. 4 confirms the validity of our classification criterion: when CL-V is used as reference, the relative amplification tends to unity at short periods for CL-II to CL-VI, and at long periods for CL-I.

The predominant-period classification shows interesting results also for class CL-I (predominant period of less than 0.2 s in H/V). The motions for this class have large amplification at short periods relative to CL-V. Zhao *et al*. (2006) assumed that their SC-I is consistent with a stiff class in a geology based classification. The cross reference between site geologic conditions and predominant period classification in our study suggests that rock weathering can play a role in high-frequency amplifications observed at rock sites. Similarly, thin-soft-layer sites (e.g. class E of CEN, 2004) can also fall in CL-I, contributing to large amplitudes. Weathered rock and class E are quite pervasive and difficult to avoid in practice, and conventional classification criteria are not able to simply recognize them.

Sites with deep soil profiles (as CL-IV sites for instance) are easily recognized in our approach, which also offers the advantage of providing quick and inexpensive site characterization without the necessity of performing time consuming and invasive analysis.

As the predominant period classification implicitly contains both velocity and thickness of the upper resonant layers in its definition, it may be intrinsically better than using V_{S30} alone. In this sense it is consistent, at least in spirit, with criteria that require the depth of soft upper layers in the site classification, as proposed by Rodriguez-Marek *et al*. (2001), Lang and Schartz (2006), Pitilakis *et al*. (2006) and Cadet *et al*. (2010).

However, being based on the predominant period and not on the fundamental period for the whole sediment cover, the proposed method could suffer from potential limitations in situations where the largest impedance contrast is at shallow depths, with significant velocity variations at greater depths. One of these cases is provided by the station GBP. This station is installed in the middle of the Gubbio basin over several hundred meters of sediments, with a fundamental frequency of resonance <0.5 Hz (Bindi *et al*., 2009b); in this instance, since the vertical component is strongly affected by surface waves generated in the basin, the H/V fails to capture the strong site amplifications below 1 Hz, even if the fundamental frequency of resonance is seen on the H/V ratio. Additionally, by limiting the analysis to periods less than 2 seconds, the proposed method is not be suitable for sites where the predominant period is greater than threshold.

Comment [DBP1]: I do not understand what you are saying in this sentence. How can H/V detect the fundamental resonance at a frequency less than 0.5 Hz yet not capture the amplification below 1 Hz? And how can H/V detect a f0<0.5 Hz if the analysis is limited to f>= 0.5 Hz?

Notwithstanding these possible limitations, an additional advantage of the proposed method relies on the fact that we find a good degree of similarity of our derived GMPEs to those using many more data from other parts of the world, even though deriving GMPEs was not a main goal for this paper.

Finally, we believe that future work should be done to explore the feasibility of using ambient noise to estimate predominant period from Fourier H/V spectral ratios, thus allowing classification of sites with no earthquake recordings.

Data and Resources

The strong-motion data used in this study have been recorded by the Rete Accelerometrica Nazionale (RAN). The data, as well as their metadata, are available through the Italian Accelerometric Archive (ITACA Working Group 2009) at

http://itaca.mi.ingv.it/ItacaNet/. Both corrected (Massa *et al*., 2009) and uncorrected waveforms are available for download.

ITACA is the Italian strong-motion database, developed from 2004 in the framework of the 2004-2006 DPC-INGV agreement and includes strong-motion data (1972-2004) from the National Accelerometer Network (RAN), presently operated by the Dipartimento Protezione Civile (DPC) (http://www.protezionecivile.it); the database includes as well revised earthquakes, recording sites and instrument metadata. An updated and improved release of ITACA is currently under construction, including strong-motion data from 2005 to 2007 and records from the latest major earthquake occurred in Italy (the 2008, M 5.1, Parma earthquake and the 2009 L'Aquila seismic sequence).

The supplemental velocity-sensor (Trillium 40-s) seismograms for the selected recent events with Mw > 4.0 were recorded by seismological stations of the Italian Seismic Network run by Istituto Nazionale di Geofisica e Vulcanologia (INGV). These waveforms are available at http://iside.rm.ingv.it.

Origin times, epicenters location and focal parameters of earthquakes are from the INGV-CNT website at http://cnt.rm.ingv.it.

More general information on site classification adopted for the strong-motion stations can be found on the DPC-INGV S4 project at http://esse4.mi.ingv.it.

Acknowledgments

This study began as a part of a Cooperative Agreement between IRSN and INGV for the years 2005-2007 and continued in Project S4 funded by Department of Civil Protection of Italy for the years 2007-2010 (http://esse4.mi.ingv.it). C.D.A. was supported by a fellowship from this project. She spent two years as a visiting scientist at the USGS, Menlo Park, CA, and is currently a post-doctoral fellow at PEER, UC

Berkeley, CA. We thank the project co-directors, Francesca Pacor and Roberto Paolucci for their continuous encouragement. The authors acknowledge Antonella Gorini for the assistance in processing the strong-motion data. John Zhao provided the code for the evaluation of his ground-motion prediction equations. Marco Moro provided the GIS-base for the simplified soil classification of the Italian territory, and Giuseppe Di Capua helped with the soil characterization for some stations by means of cooperative information exchange. We also want to thank Giovanna Calderoni, Fabrizio Cara, Giuseppe Di Giulio and Giuliano Milana for discussions and useful computational advice. Finally, we thank Dino Bindi, J.B. Fletcher, yyy, and zzz for useful reviews that improved the manuscript.

References

Abrahamson, N. A. and W.J. Silva (1997). Empirical response spectral attenuation relations for shallow crustal earthquakes, *Seismol. Res. Lett.*, 68, 94–127.

Akinci, A., L. Malagnini, F. Sabetta (2010). Characteristics of the strong ground motions from the 6 April 2009 L'Aquila earthquake, Italy, *Soil Dynamics and Earthquake Engineering*, 30, 320–335.

Akkar, S. and J.J. Bommer (2006). Influence of long-period filter cut-off on elastic spectral displacements. *Earthquake Eng. Struct. Dyn*., 35, 1145–1165.

Ambraseys, N.N., J. Douglas, S.K. Sarma, and P. Smit (2005). Equations for the estimation of strong ground motions from shallow crustal earthquakes using data from Europe and the Middle East: horizontal peak ground acceleration and spectral acceleration. *Bull. Earthquake Eng.*, 3, 1–53.

Ameri, G., M. Massa, D. Bindi, E. D'Alema, A. Gorini, L. Luzi, S. Marzorati, F. Pacor, R. Paolucci, R. Puglia, and C. Smerzini (2009). The 6 April 2009, Mw 6.3, L'Aquila (Central Italy) earthquake: strong-motion observations, *Seism. Res. Lett.*, 36, 951 - 966, doi: 10.1785/gssrl.80.6.951.

Anzidei, M., E. Boschi, V. Cannelli, R. Devoti, A. Esposito, A. Galvani, D. Melini, G. Pietrantonio, F. Riguzzi, V. Sepe, and E. Serpelloni (2009). Coseismic deformation of the destructive April 6, 2009 L'Aquila earthquake (central Italy) from GPS data, *Geophys. Res. Lett.*, 36, L17307, doi:10.1029/2009GL039145.

Atzori, S., I. Hunstad, M. Chini, S. Salvi, C. Tolomei, C., Bignami, S. Stramondo, E. Trasatti, A. Antonioli, and E. Boschi (2009), Finite fault inversion of DInSAR coseismic displacement of the 2009 L'Aquila earthquake (Central Italy), *Geoph. Res. Lett.*, doi: 10.1029/2009GL039293

Bindi, D., F. Pacor, L. Luzi, M. Massa, and G. Ameri (2009a). The Mw 6.3, 2009 L'Aquila earthquake: source, path, and site effects from spectral analysis of strong motion data, *Geophys. J. Int.*, doi:10.1111/j.1365-246X.2009.04392.x.

Bindi, D., S. Parolai, F. Cara, G. Di Giulio, G. Ferretti, L. Luzi, G. Monachesi, F. Pacor, and A. Rovelli (2009b). Site amplifications observed in the Gubbio Basin, Central Italy: hints for lateral propagation effects. *Bull. seism. Soc. Am*., 99(2A):741–760

Bindi, D., L. Luzi, M. Massa, and F. Pacor (2010). Horizontal and vertical ground motion prediction equations derived from the Italian Accelerometric Archive (ITACA), *Bull. Earthquake Eng.*, doi:10.1007/s10518-009-9130-9.

Boore, D. M. (2004). Can site response be predicted?, *Journal of Earthquake Engineering*, 8, Special Issue 1, 1–41

Boore, D. M. (2005). On pads and filters: processing strong-motion data, *Bull. Seism. Soc. Am.*, 95, 745–750.

Boore, D.M., and M.W. Asten (2008). Comparisons of Shear-Wave Slowness in the Santa Clara Valley, California, Using Blind Interpretations of Data from Invasive and Noninvasive Methods, *Bull. Seism. Soc. Am.*, 98, 1983-2003.

Boore, D. M. and G. M. Atkinson (2008). Ground-motion prediction equations for the average horizontal component of PGA, PGV, and 5%-damped PSA at spectral periods between 0.01 s and 10.0 s, *Earthquake Spectra*, 24, 99-138

Boore, D. M., and J. J. Bommer (2005). Processing of strong-motion accelerograms: needs, options and consequences, *Soil Dyn. Earthq. Eng.*, 25, 93-115.

Boore, D. M., C. D. Stephens, W. B. Joyner (2002). Comment on Baseline Correction of Digital Strong-Motion Data: Examples from the 1999 Hector Mine, California, Earthquake. *Bull. Seism. Soc. Am.*, 92, 1543-1560.

Building Seismic Safety Council (2000). The 2000 NEHRP Recommended Provisions for New Buildings and Other Structures: Part I (Provisions) and Part II (Commentary), FEMA 368/369, *Federal Emergency Management Agency*, Washington, D.C.

Cadet, H., P.Y. Bard, A. Rodriguez-Marek (2010). Defining a Standard Rock Site: Propositions Based on the KiK-net Database. *Bull. Seism. Soc. Am.*, 100, 172-195.

Cara, F., G. Di Giulio, and A. Rovelli (2003). A study on seismic noise variations at Colfiorito, central Italy: implications for the use of H/V spectral ratios. *Geophys. Res. Lett.*, 30 (18), 1972.

Cara, F., G. Di Giulio, G. Milana, P. Bordoni, J. Haines, and A. Rovelli (2010). On the stability and reproducibility of the horizontal-to-vertical spectral ratios on ambient noise: the case study of Cavola, northern Italy, *Bull. Seism. Soc. Am.*, 100, 1263–1275, doi: 10.1785/0120090086

Cauzzi, C., and E. Faccioli (2008). Broadband (0.05 to 20 s) prediction of displacement response spectra based on worldwide digital records, *J. Seismol.*, doi: 10.1007/s10950-008-9098-y.

Çelebi, M., P. Bazzurro, L. Chiaraluce, P. Clemente, L. Decanini, A. DeSortis, W. Ellsworth, A. Gorini, E. Kalkan, S. Marcucci, G. Milana, F. Mollaioli, M. Olivieri, R. Paolucci, D. Rinaldis, A. Rovelli, F. Sabetta and C. Stephens (2010). Recorded Motions of the Mw6.3 April 6, 2009 L'Aquila (Italy) Earthquake and Implications for Building Structural Damage: A Review, *Earthquake Spectra*, 23, 651–684, doi: 10.1193/1.3450317.

CEN, European Committee for Standardization (2004). Eurocode 8: design of structures for earthquake resistance - part 1: general rules, seismic actions and rules for buildings. Bruxelles.

Chiarabba, C., P. De Gori, L. Chiaraluce, P. Bordoni, M. Cattaneo, M. De Martin, A. Frepoli, A. Michelini, A. Monachesi, M. Moretti, G. P. Augliera, E. D'Alema, M. Frapiccini, A. Gassi, S. Marzorati, P. Di Bartolomeo, S. Gentile, A. Govoni, L. Lovisa, M. Romanelli, G. Ferretti, M. Pasta, D. Spallarossa, and E. Zumino (2005). Mainshocks and aftershocks of the 2002 Molise seismic sequence, southern Italy*, J. Seismol.*, 9, 487-494.

Chiarabba, C., A. Amato, M. Anselmi, P. Baccheschi, I. Bianchi, M. Cattaneo, G. Cecere, L. Chiaraluce, M.G. Ciaccio, P. De Gori, G. De Luca, M. Di Bona, R. Di Stefano, L. Faenza, A. Govoni, L. Improta, F.P. Lucente, A. Marchetti, L. Margheriti, F. Mele, A. Michelini, G. Monachesi, M. Moretti, M. Pastori, M. Piana Agostinetti, D. Piccinini, P. Roselli, D. Seccia, and L. Valoroso (2009). The 2009 L'Aquila (central

Italy) MW6.3 earthquake: Main shock and aftershocks, *Geophys. Res. Lett.*, 36, L18308, doi:10.1029/2009GL039627.

Chioccarelli, E., and I. Iervolino (2010). Near-source seismic demand and pulse-like records: A discussion for L'Aquila earthquake, *Earthquake Engng. Struct. Dyn.*, doi: 10.1002/eqe.987.

Cirella, A., A. Piatanesi, M. Cocco, E. Tinti, L. Scognamiglio, A. Michelini, A. Lomax, and E. Boschi (2009), Rupture history of the 2009 L'Aquila earthquake from non-linear joint inversion of strong motion and GPS data, *Geophys. Res. Lett.* 36, L19304, doi:10.1029/2009GL039795

Cocco, M., and A. Rovelli (1989). Evidence of the variation of stress drop between normal and thrust faulting earthquakes in Italy, *J. Geoph. Res.*, 94, 9399 – 9416.

Converse, A. M., and A. G. Brady (1992). BAP - basic strong-motion accelerogram processing software; Version 1.0. *United States Geological Survey Open-File Report*, 174; 92–296A.

De Luca, G., S. Marcucci, G. Milana, and T. Sano' (2005). Evidence of Low-Frequency Amplification in the City of L'Aquila, Central Italy, through a Multidisciplinary Approach Including Strong- and Weak-Motion Data, Ambient Noise, and Numerical Modeling. *Bull. Seism. Soc. Am.*, 95, 1469-1481.

Di Alessandro, C., A. Rovelli, G. Milana, S. Marcucci, L.F. Bonilla, and D.M. Boore (2009). A New Site Classification Scheme for Italian Accelerometric Stations, in the 2009 SSA Annual Meeting, Monterey, CA, USA, 8-10 April 2009, paper n.63

Di Capua G., Lanzo G., Peppoloni S., Pessina V., Scasserra G. (2011).The ITACA recording stations: general information and site classification, *Bull Earthq. Eng*. (submitted)

Di Giulio, G., C. Cornou, M. Ohrnberger, M. Wathelet, and A. Rovelli (2006). Deriving wavefield characteristics and shear-velocity profiles from two-dimensional small-aperture arrays analysis of ambient vibrations in a small-size alluvial basin, Colfiorito, Italy, *Bull. Seism. Soc. Am.*, 96, 1915-1933, doi: 10.1785/0120060119.

Ekström, G., A. Morelli, E. Boschi, and A. M. Dziewonski (1998). Moment tensor analysis of the central Italy earthquake sequence of September–October 1997, *Geophys. Res. Lett.*, 25, 1971–1974.

Fukushima Y. and T. Tanaka (1990). A new attenuation relation for peak horizontal acceleration of strong earthquake ground motion in Japan, *Bull. Seism. Soc. Am.*, 80, 757-783.

Fukushima Y., C. Berge-Thierry, P. Volant, D. A. Griot-Pommera, and F. Cotton (2003). Attenuation relation for west Eurasia determined with recent near-fault records from California, Japan and Turkey, *J. Earthq Eng.*, 7, 1-26.

Fukushima Y., L. F. Bonilla, O. Scotti, and J. Douglas (2007). Site classification using horizontal-to-vertical response spectral ratios and its impact when deriving empirical ground-motion prediction equations, *J. Earthq Eng.*, 11, 712-724.

Ghasemi, H., M. Zare, Y. Fukushima, F. Sinaeian (2009). Applying empirical methods in site classification, using response spectral ratio (H/V): A case study on

Iranian strong motion network (ISMN), *Soil Dynamics and Earthquake Engineering*, 29, 121–132

Guillier, B., J.-L. Chatelain, S. Bonnefoy-Claudet, E. Haghshenas (2007). Use of Ambient Noise: From Spectral Amplitude Variability to H/V Stability, *J. Earthq Eng.*, 11 (6), 925-942.

Japan Road Association (1980). Specifications for Highway Bridges Part V, Seismic Design, Maruzen Co., LTD.

Japan Road Association (1990). Specifications for Highway Bridges Part V, Seismic Design, Maruzen Co., LTD

Joyner, W. B. and D. M. Boore (1993). Methods for regression analysis of strong-motion data, *Bull. Seism. Soc. Am.*, 83, 469-487.

Lang, D.H. and Schwarz, J. (2006): Instrumental subsoil classification of Californian strong-motion sites based on single-station measurements. *Proceedings of the Eighth U.S. National Conference on Earthquake Engineering*, San Francisco, United States, 2006.

Luzi L., Sabetta F., Hailemikael S., Bindi D., Pacor F., and F. Mele (2008). ITACA (ITalian ACcelerometric Archive): a web portal for the dissemination of Italian strong motion data. *Seism. Res. Lett.* 79(5): 717–723. doi:10. 1785/gssrl.79.5

Luzi L., M. Gallipoli, M.Mucciarelli D. Bindi and F. Pacor (2011). Testing of diffrent seismic parameters for seismic parameters for site classification. Submitted to *Bull. Earthq. Eng*.

Malagnini, L., A. Rovelli, S. E. Hough, and L. Seeber (1993). Site amplification estimates in the Garigliano valley, central Italy, based on dense array measurements of ambient noise, *Bull. Seism. Soc. Am.*, 83, 1744-1755.

Massa, M., F. Pacor, L. Luzi, D. Bindi, G. Milana, F. Sabetta, A. Gorini, and S. Marcucci (2009). The ITalian ACcelerometric Archive (ITACA): processing of strong-motion data, *Bull. Earthq. Eng.*, D.O.I. 10.1007/s10518-009-9152-3

Mucciarelli M., M.R. Gallipoli, and M. Arcieri (2003). The stability of Horizontal-to-Vertical Spectral Ratio by triggered noise and earthquake recordings, *Bull. Seism. Soc. Am.*, 93, 1407-1412.

Pacor F., R. Paolucci, A. De Sortis, A. Gorini and A. Spinelli (2011). Overview of the Italian strong motion database 1.0. Submitted to *Bull Earthq. Eng*.

Paolucci, R., A. Rovelli, E. Faccioli, C. Cauzzi, D. Finazzi, M. Vanini, C. Di Alessandro, and G. Calderoni (2008). On the reliability of long period response spectra ordinates from digital accelerograms, *Earthquake Engng. Struct. Dyn.*, 37, 697–710.

Park, D. and Y.M.A. Hashash (2004). Probabilistic seismic hazard analysis with non linear site effects in the Mississippi embayment, *Proc. 13th World Conf. Earthq. Eng*, Vancouver, CD-Rom Edition, paper n. 1549.

Pino, N.A., and F. Di Luccio (2009). Source complexity of the 6 April 2009 L'Aquila (central Italy) earthquake and its strongest aftershock revealed by elementary seismological analysis, *Geophys. Res. Lett.*, 36, /L23305, doi:10.1029/2009GL041331.

Pitilakis, K., C. Gazepis, and A. Anastasiadis (2006). Design response spectra and soil classification for seismic code provisions, in Proc. of the Athens Workshop, Geotechnical Evaluation and Application of the Seismic Eurocode EC8, 31–46.

Pondrelli, S., G. Ekström, and A. Morelli (2001). Seismotectonic re-evaluation of the 1976 Friuli, Italy, seismic sequence, *Journal of Seismology*, 5, 73-83.

S4 project – Deliverable D8 (2009). Progress report on Identification of ITACA sites and records with distinctive features in their seismic response., May 2009. Available from http://esse4.mi.ingv.it/.

Rodriguez-Marék, A., J. D. Bray, and N. A. Abrahamson (2001). An empirical geotechnical seismic site response procedure, *Earthquake Spectra*, 17, 65–87.

Scasserra, G., J.P. Stewart, P. Bazzurro, G. Lanzo, and F. Mollaioli (2009). A Comparison of NGA Ground-Motion Prediction Equations to Italian Data, *Bull. Seism. Soc. Am.*, 99(5), 2961–2978, doi: 10.1785/0120080133

Scherbaum, F., J. Schmedes, and F. Cotton (2004). On the conversion of source-to-site distance measures for extended earthquake source models, *Bull. Seism. Soc. Am.*, 94, 1053-1069.

SESAME Project – Deliverable D23.12 – Guidelines for the implementation of the H/V spectral ratio technique on ambient vibration measurement, processing and interpretation: http://sesame-fp5.obs.ujf-grenoble.fr/Delivrables/Del-D23_HV_User_Guidelines.pdf, 2005.

Spudich, P., W. B. Joyner, A. G. Lindh, D. M. Boore, B. M. Margaris, and J.B Fletcher (1999). SEA99: a revised ground motion prediction relation for use in extensional tectonic regimes, *Bull. Seism. Soc. Am.*, 89, 1156–70.

Steidl, J.H. (2000). Site Response in Southern California for Probabilistic Seismic Hazard Analysis. Bull. Seism. Soc. Am., 90, 149 – 169.

Working Group ITACA (2009) - Data Base of the Italian strong motion records: http://itaca.mi.ingv.it

Xia, J., R.D. Miller, C.B. Park, J.A. Hunter, J.B. Harris, and J. Ivanov (2002). Comparing shear-wave velocity profiles from multichannel analysis of surface wave with borehole measurements, *Soil Dyn. Earthq. Eng.*, 22, 181-190.

Yamazaki, F., and M. A. Ansary (1997). Horizontal-to-vertical spectrum ratio of earthquake ground motion for site characterization, *Earthquake Eng. Struct. Dyn.* 26, 671–689.

Zhao, J. X., K. Irikura, J. Zhang, Y. Fukushima, P. G. Somerville, T. Saiki, H. Okada, and T. Takahashi (2004). Site classification for strong-motion stations in Japan using H/V response spectral ratio, in *13th World Conference of Earthquake Engineering*, Vancouver, B.C., Canada, 1–6 August 2004, paper no. 1278.

Zhao, J. X., K. Irikura, J. Zhang, Y. Fukushima, P. G. Somerville, A. Asano, Y. Ohno, T. Oouchi, T. Takahashi and H. Ogawa (2006), An Empirical Site-Classification Method for Strong-Motion Stations in Japan Using H/V Response Spectral Ratio, *Bull. Seism. Soc. Am.*, 96, 914-925.

Affiliations and Contact Information

Pacific Earthquake Engineering Research Center (PEER)
325 Davis Hall, University of California, Berkeley,
University of California, Berkeley, CA 94720-1792
carola.dialessandro@berkeley.edu
(C.D.A.)

Institut Français des Sciences et Technologies des Transports de l'Aménagement et des Réseaux (IFSTTAR)
Département Géotechnique, Eau et Risques - Groupe Séismes et Vibrations
58 boulevard Lefebvre
75732 Paris Cedex 15
fabian.bonilla@lcpc.fr
(L.F.B)

U.S. Geological Survey
MS 977
345 Middlefield Road
Menlo Park, California 94025
boore@usgs.gov
(D.M.B.)

Istituto Nazionale di Geofisica e Volcanologia (INGV)
Via di Vigna Murata, 605
00143 Roma, Italy
antonio.rovelli@ingv.it
(A.R)

Institute for Radiological protection and Nuclear Safety (IRSN)
31, avenue de la Division Leclerc
92260 Fontenay-aux-Roses, France
oona.scotti@irsn.fr
(O.S)

Tables

Table 1: Classification criteria based on V_{S30} and soil properties for European Seismic Code classes (CEN, 2000) and NEHRP scheme (BSSC, 2000).

CLASS	Average Shear-Wave Velocity (V_{S30}) (m/s)	
	NEHRP	CEN
A	> 1500	> 800
B	760 – 1500	360 – 800
C	360 – 760	180 – 360
D	180 – 360	< 180
E	< 180	Surface alluvium layer with Vs values of type C or D and thickness between 5 and 20 m, underlain by stiffer material with Vs > 800 m/s

Table 2: Comparison among the class definition criteria adopted for the predominant period classifications in Zhao *et al*. (2006), Fukushima *et al*. 2007 and this study. Tg is the site natural period (in seconds) as inferred from the H/V spectral ratios.

Site Class – Zhao *et al*. (2006)		Site Class – Fukushima *et al*. (2007)		Site Class - our proposal	
SC-I	Tg < 0.2 sec.	SC-1	Tg < 0.2 sec.	CL-I	Tg < 0.2 sec.
SC-II	0.2 sec. ≤ Tg < 0.4 sec.	SC-2	0.2 sec. ≤ Tg < 0.6 sec.	CL-II	0.2 sec. ≤ Tg < 0.4 sec.
SC-III	0.4 sec. ≤ Tg < 0.6 sec.			CL-III	0.4 sec. ≤ Tg < 0.6 sec.
SC-IV	0.6 sec. ≤ Tg	SC-3	0.6 sec. ≤ Tg	CL-IV	0.6 sec. ≤ Tg
		SC-4	Tg not identifiable and original Rock site	CL-V	Tg not identifiable (flat H/V and amplitude < 2)
		SC-5	Tg not identifiable and original Soil site	CL-VI	broad amplification / multiple peaks @ Tg > 0.2 sec.
				CL-VII	Tg not identifiable (multiple peaks over entire period range)

Table 3: Simplified classification and its correspondence with standard classification based on V_{S30} for European Seismic Code classes (CEN, 2000) and NEHRP scheme (BSSC, 2000).

Combined Soil Classes	Average Shear-Wave Velocity (V_{S30})	CEN Classes	NEHRP Classes
AB	$V_{S30} \geq 360$ m/s	A, B and E	B + C
CD	$V_{S30} < 360$ m/s	C and D	D + E

Table 4: Cross-tabulation of stations into the two sets of site classes.

NUMBER OF STATIONS								
	CL-I	CL-II	CL-III	CL-IV	CL-V	CL-VI	CL-VII	TOT
AB	19	19	16	11	11	3	12	91
CD	3	2	2	9	0	2	2	20
TOT	22	21	18	20	11	5	14	111

Table 5: Cross-tabulation of records into the two sets of site classes.

NUMBER OF RECORDS								
	CL-I	CL-II	CL-III	CL-IV	CL-V	CL-VI	CL-VII	TOT
AB	142	90	72	45	73	12	58	492
CD	13	23	7	46	0	14	7	110
TOT	155	113	79	91	73	36	65	602

Table 6: Number of records in each moment magnitude group.

NUMBER OF RECORDS for Mw Class				
	Mw < 5.0	Mw: 5.0 – 5.4	Mw: 5.5 – 5.9	Mw >5.9
CL-I	84	36	28	7
CL-II	62	20	21	10
CL-III	40	22	10	7
CL-IV	35	12	32	12
CL-V	36	13	16	8
CL-VI	7	3	12	4
AB	253	99	96	44
CD	47	24	30	9

Table 7: Number of records in each hypocentral distance group.

NUMBER OF RECORDS for R Hypo Class			
	R Hypo < 50 km	R Hypo: 50 – 100 km	R Hypo > 100 km
CL-I	130	13	12
CL-II	96	14	3
CL-III	53	17	9
CL-IV	52	27	12
CL-V	48	10	15
CL-VI	16	7	3
AB	354	78	60
CD	85	19	6

Figure captions

Figure 1: Proposed classification criterion based on the predominant period identified from the average H/V spectral ratio (black solid line) of the 5%-damped response spectra recorded at each site (red curves). An example is provided for accelerometer station sites (whose name is displayed at the up right corner of each panel) that fall into the various classes. The light blue shaded area indicates the interval of validity in which each class is defined.

Figure 2: Distribution of moment magnitude and hypocentral distance for the selected dataset. Different symbols correspond to the predominant period classification scheme proposed in this study.

Figure 3: (a) Geometric mean H/V response spectral ratio for each site class proposed in this study, and (b) standard deviations in natural logarithm units.

Figure 4: (a) Relative amplification of predominant period site classes with respect to class CL-V, as well as of CD with respect to AB. (b) Mean ± 1 standard deviation of the relative amplification of AB and CD sites with respect to CL-V as obtained from averaging different scenarios compatible with our dataset. Relative amplification of CD versus in AB is also shown for comparison.

Figure 5: Predicted response spectra for the classification proposed in this study, compared to Zhao *et al*. (2006), Fukushima *et al*. (2007), whose nomenclature of the site classes is described in Table 2. Spectral ordinates are for moment magnitudes Mw 4.5 and 6.0 (panels from top to the bottom) at hypocentral distance 50 km. Predicted spectra according to Zhao *et al*. (2006) were evaluated for earthquake scenario with focal depths

less than 15 km and for unspecified fault type. “PER. AMPL.” is the abbreviation for period amplification; site classes that amplify at short periods or have a rock -like behavior are shown in the left panel, site classes that amplify at intermediate periods or have a shallow-soil - like behavior are shown in the central panel, and site classes that amplify at long periods or have a deep-soil - like behavior are shown in the right panel.

Figure 6: (a) Overall standard deviation obtained using predominant period classification and original simplified AB and CD site classes in decimal logarithms. Inter and intra-event terms are also shown for the predominant period classification scheme. (b) Overall standard deviations from Bindi *et al*., 2010 and Fukushima *et al*., 2007 in the same units as above are also provided for comparison. The curve for Fukushima *et al*. (2007) referring to their original rock / soil classification has been kindly provided by the author and allows to evaluate the reduction in standard deviation those authors achieved when adopting predominant period classification, analogously to what we show in panel (a).

Figure 7: Residuals of PGA and spectral ordinates at 0.2 and 1.0 sec periods during the April 6, 2009, Mw 6.3 L’Aquila earthquake. In the panels showing the residuals of predominant-period classes, cross and open circle symbols are used to distinguish stations with source back-azimuth affected by anti-directive and directive effects (i.e. whose source-to-station azimuth measured clockwise from north is in the range 57° – 187° and 200° – 330°, respectively).

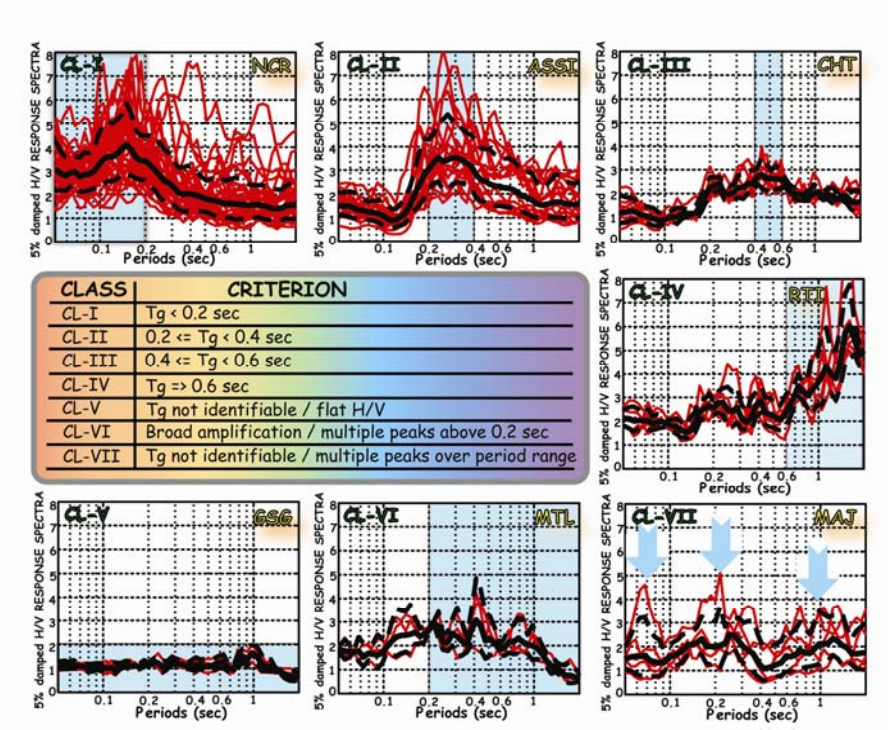

Figure 1: Proposed classification criterion based on the predominant period identified from the average H/V spectral ratio (black solid line) of the 5%-damped response spectra recorded at each site (red curves). An example is provided for accelerometer station sites (whose name is displayed at the up right corner of each panel) that fall into the various classes. The light blue shaded area indicates the interval of validity in which each class is defined.

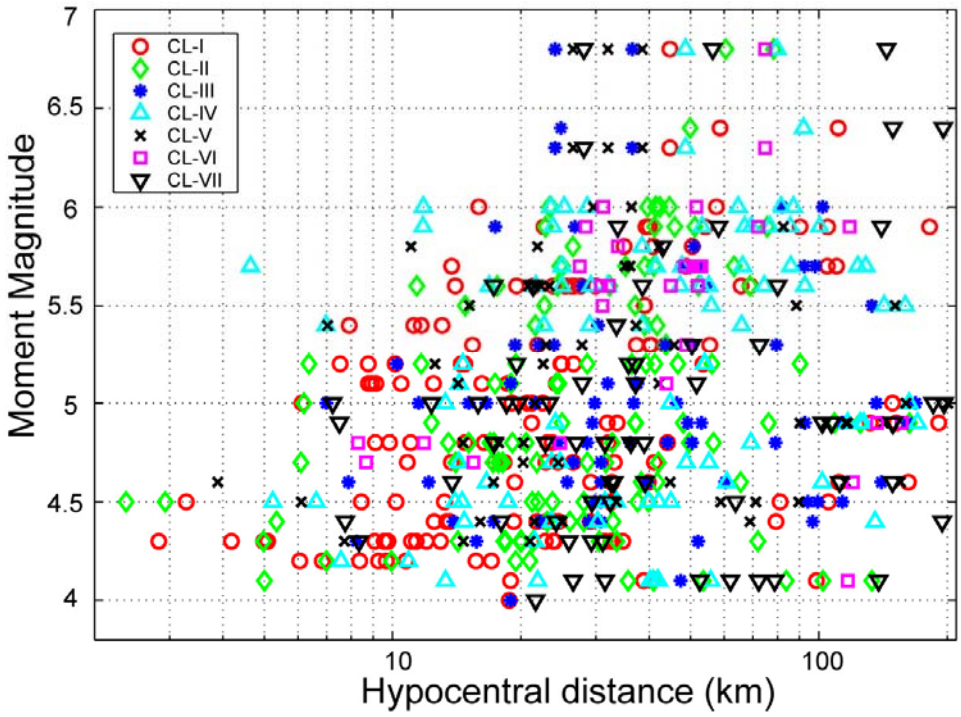

Figure 2: Distribution of moment magnitude and hypocentral distance for the selected dataset. Different symbols correspond to the predominant period classification scheme proposed in this study.

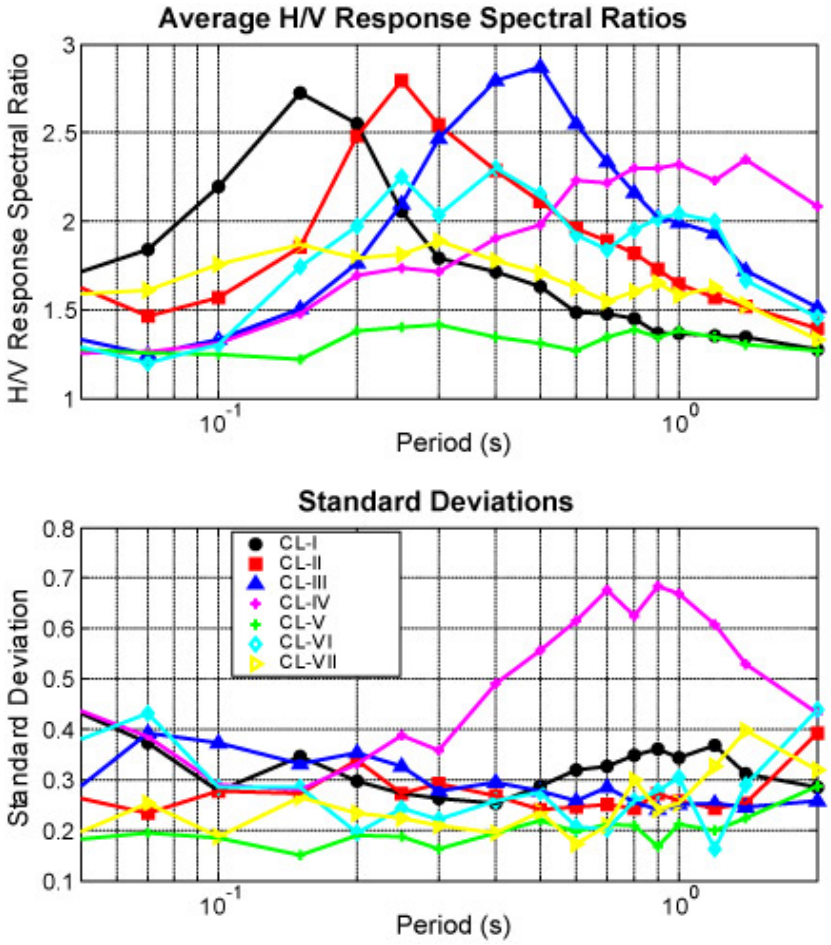

Figure 3: (a) Geometric mean H/V response spectral ratio for each site class proposed in this study, and (b) standard deviations in natural logarithm units.

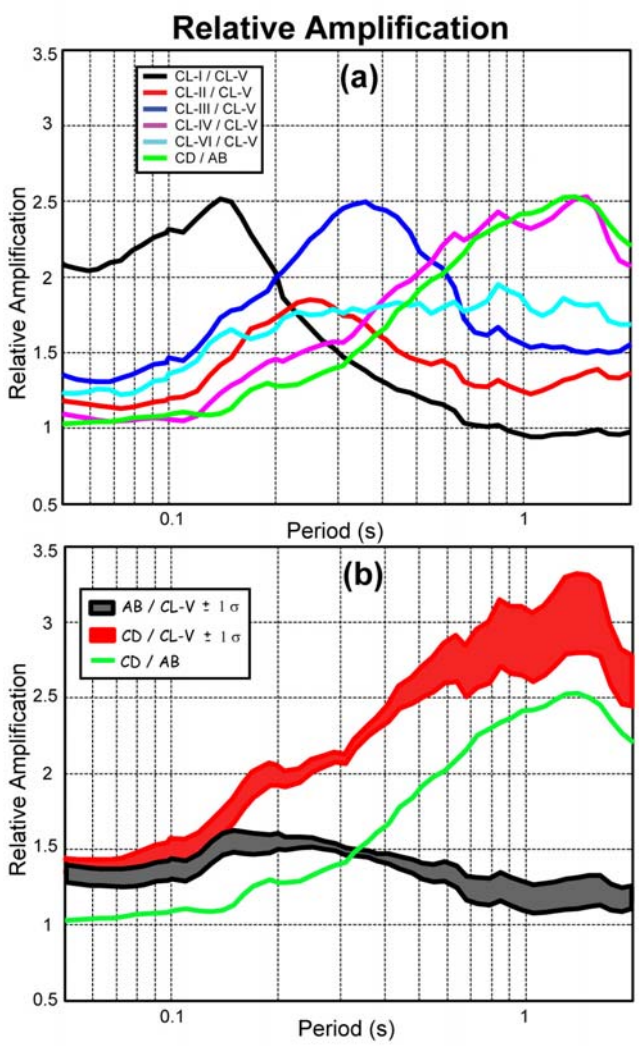

Figure 4: (a) Relative amplification of predominant period site classes with respect to class CL-V, as well as of CD with respect to AB. (b) Mean ± 1 standard deviation of the relative amplification of AB and CD sites with respect to CL-V as obtained from averaging different scenarios compatible with our dataset. Relative amplification of CD versus in AB is also shown for comparison.

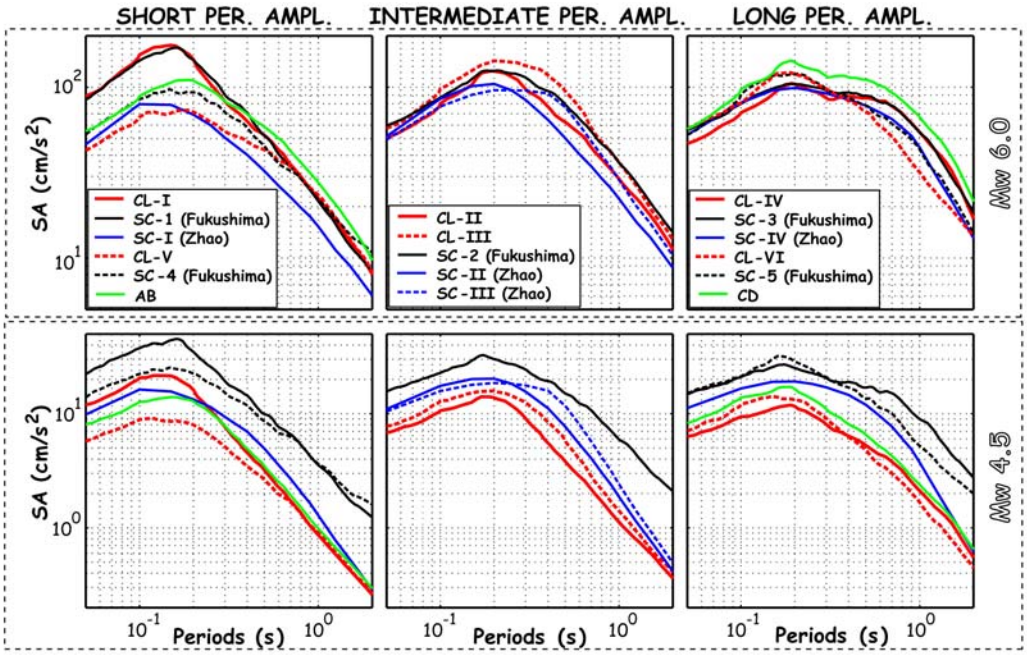

Figure 5: Predicted response spectra for the classification proposed in this study, compared to Zhao *et al*. (2006), Fukushima *et al*. (2007), whose nomenclature of the site classes is described in Table 2. Spectral ordinates are for moment magnitudes Mw 4.5 and 6.0 (panels from top to the bottom) at hypocentral distance 50 km. Predicted spectra according to Zhao *et al*. (2006) were evaluated for earthquake scenario with focal depths less than 15 km and for unspecified fault type. "PER. AMPL." is the abbreviation for period amplification; site classes that amplify at short periods or have a rock -like behavior are shown in the left panel, site classes that amplify at intermediate periods or have a shallow-soil - like behavior are shown in the central panel, and site classes that amplify at long periods or have a deep-soil - like behavior are shown in the right panel.

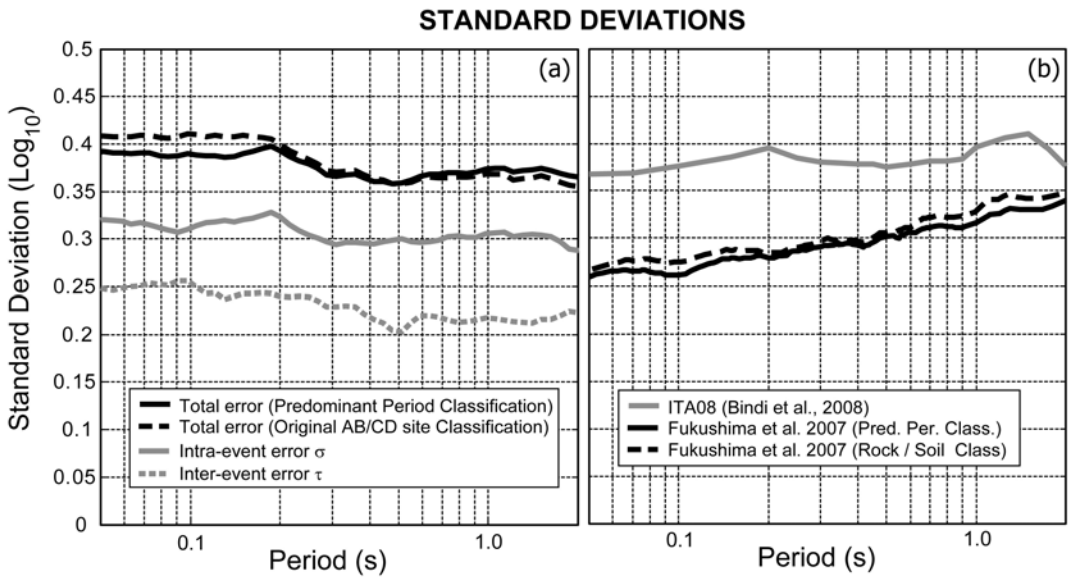

Figure 6: (a) Overall standard deviation obtained using predominant period classification and original simplified AB and CD site classes in decimal logarithms. Inter and intra-event terms are also shown for the predominant period classification scheme. (b) Overall standard deviations from Bindi *et al*., 2010 and Fukushima *et al*., 2007 in the same units as above are also provided for comparison. The curve for Fukushima *et al*. (2007) referring to their original rock / soil classification has been kindly provided by the author and allows to evaluate the reduction in standard deviation those authors achieved when adopting predominant period classification, analogously to what we show in panel (a).

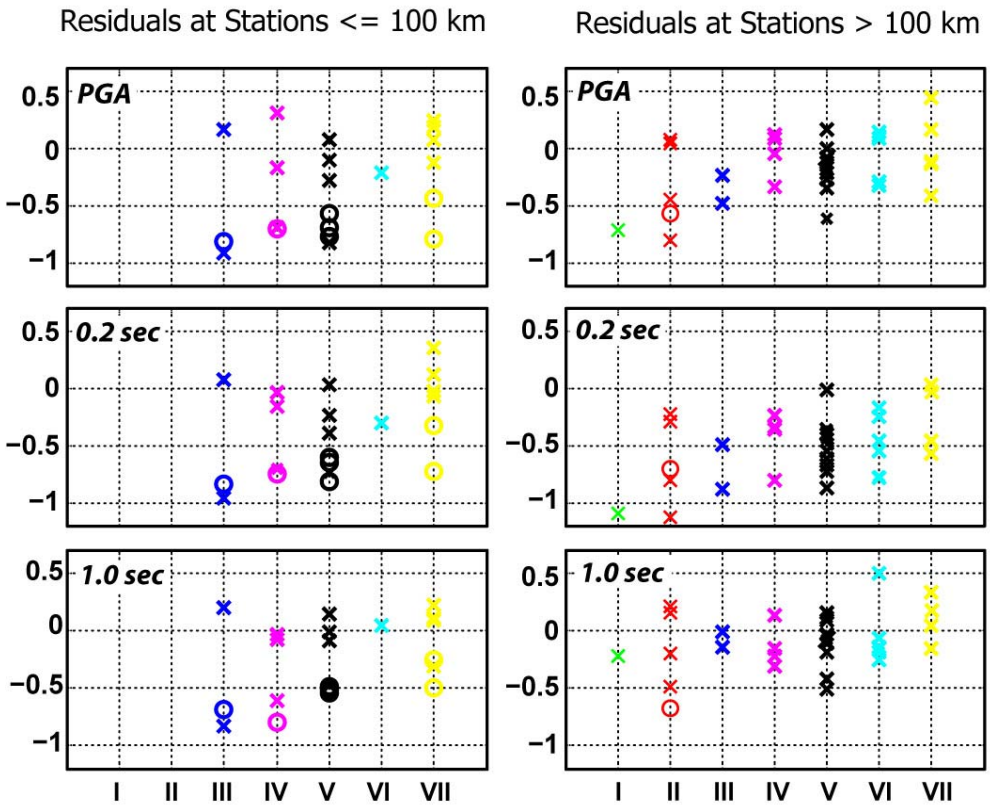

Figure 7: Residuals of PGA and spectral ordinates at 0.2 and 1.0 sec periods during the April 6, 2009, Mw 6.3 L'Aquila earthquake. In the panels showing the residuals of predominant-period classes, cross and open circle symbols are used to distinguish stations with source back-azimuth affected by anti-directive and directive effects (i.e. whose source-to-station azimuth measured clockwise from north is in the range 57° – 187° and 200° – 330°, respectively).